Supporting Information for

Journal of Microscopy, Vol. 234, Pt 1 2009, pp. 38–46
Received 4 October 2008; accepted 7 November 2008

TIRF microscopy evanescent field calibration using tilted fluorescent microtubules

C. GELL*,‡, M. BERNDT*,‡, J. ENDERLEIN† & S. DIEZ*
*Max-Planck-Institute of Molecular Cell Biology and Genetics, Dresden, Germany
†III. Institute of Physics, Georg-August-University, Göttingen, Germany

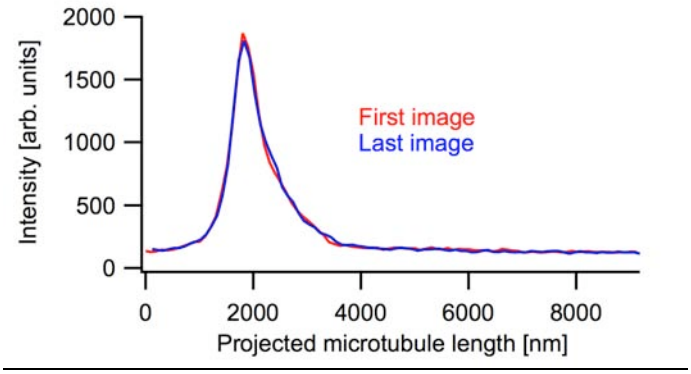

Fig. S1. The normalized intensity profile along a titled microtubule measured in TIRF for a laser AOI of 63°, before (red) and after (blue) multiple measurements at other AOIs. These data show that the reproducibility of the AOI is good and that over the time course of a typical measurement neither bleaching nor microtubule depolymerization are significant effects.

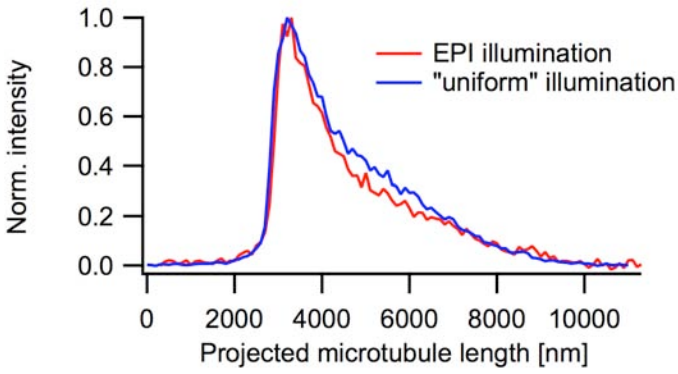

Fig. S2. Intensity profiles along a steeply tilted (approximately 15.9°) microtubule in both uniform illumination (a laser beam at 0° AOI) and with EPI illumination are nearly identical.

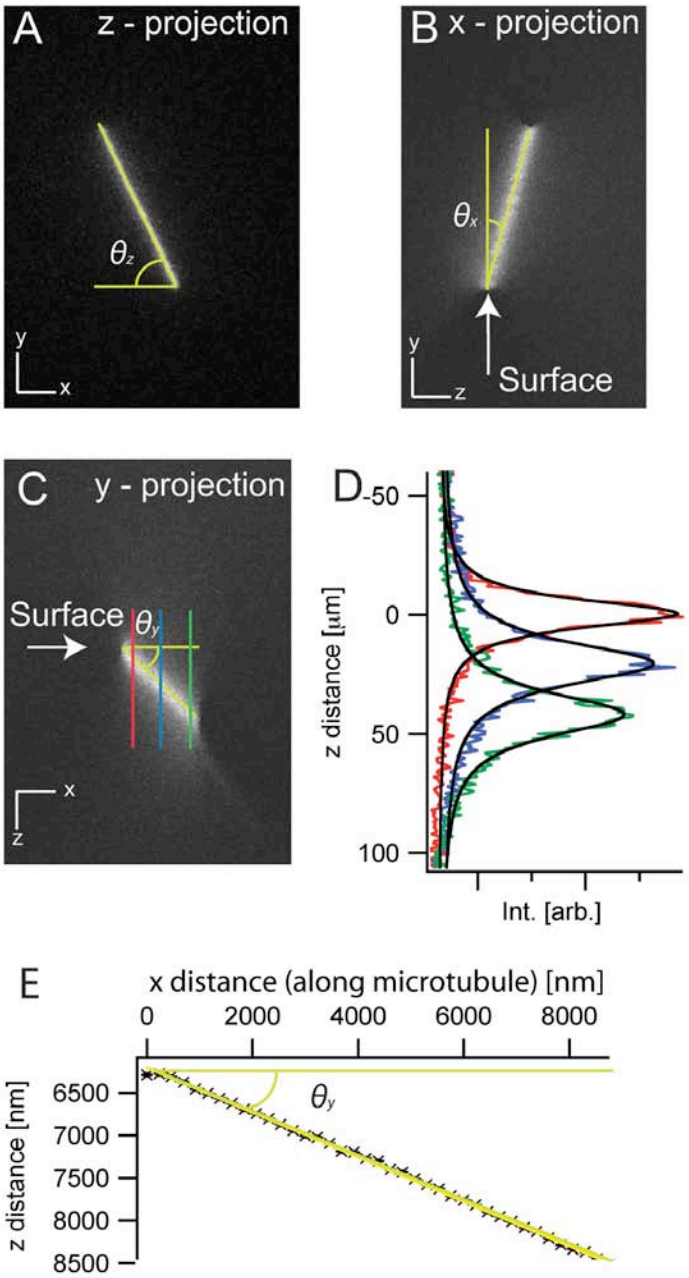

Fig. S3. Method to determine microtubule tilt angle: A *z* stack (50 nm resolution) of a tilted microtubule was recorded using EPI illumination. Maximum projections were then made in the three orthogonal directions; shown above are the **A)**: *z* projection, **B)**: *x* projection and **C)**: *y* projection. Recording the microtubule angle with respect to two orthogonal axes allows calculation of the 'apparent' tilt angle with respect to the cover glass. **D)** The microtubule's central axis is located by multiple Lorentzian fits along the microtubule (three such fits are shown for illustration, which are the line profiles and fits along the similarly coloured lines shown in C). **E)** The slope of a plot of the microtubule *z* position (Lorentzian peak tops) versus position along the microtubule (E shows the plot for the image in C) gives the tangent of the microtubule angle from that projection.

Appendix S1

Mathematical Description of Data

As explained in the main text (Equation 4) the measured fluorescence intensity I_C of an object in an image (image coordinate space; x,y,z) can be described by the convolution of the illuminated object (object coordinate space; x_0,y_0,z_0) with the 3-D point-spread-function (PSF) of the imaging system.

In our special case, the following assumptions and simplifications can be made:

1) The illumination profile is homogeneous in the x_0-y_0 plane (i.e. $I_{ex}(x_0, y_0, z_0) = I_{ex}(z_0)$).
2) The image is obtained on the camera chip at position z=0 (i.e $I_C(x,y,z=0) \Rightarrow I_C(x,y)$).
3) The microtubule has a length L and can be idealised as a uniformly labelled 1-D fluorescent object due to its sub-resolution diameter; the microtubule is aligned along the x_0-axis (at y_0=0) with tilt-angle θ_{tilt} against the x_0-y_0-plane ($z_0=x_0 \tan \theta_{tilt}$); and touches the cover slip with one end at z_0=0.

Equation 4 then simplifies to:

$$I_C(x,y) = \int_0^{L\cdot\cos\theta_{tilt}} I_{ex}\left(x_0 \tan\theta_{tilt}\right) \cdot F\left(\frac{x_0}{\cos\theta_{tilt}}\right) \cdot PSF(x - x_0, y, -x_0 \tan\theta_{tilt})\ dx_0 \qquad \text{(S1)}$$

Considering TIRF and EPI illumination with vertical profiles $I_{ex}^{TIR}(x_0 \tan\theta_{tilt})$ and $I_{ex}^{EPI}(x_0 \tan\theta_{tilt}) = I_{ex}^{EPI} = \text{constant}$, respectively, one obtains:

$$I_C^{TIR}(x,y) = \int_0^{L\cdot\cos\theta_{tilt}} I_{ex}^{TIR}\left(x_0 \tan\theta_{tilt}\right) \cdot F\left(\frac{x_0}{\cos\theta_{tilt}}\right) \cdot PSF(x - x_0, y, -x_0 \tan\theta_{tilt})\ dx_0 \qquad \text{(S2)}$$

$$I_C^{EPI}(x,y) = \int_0^{L\cdot\cos\theta_{tilt}} F\left(\frac{x_0}{\cos\theta_{tilt}}\right) \cdot PSF(x - x_0, y, -x_0 \tan\theta_{tilt})\ dx_0 \qquad \text{(S3)}$$

For further simplification, we effectively reduce the camera image to a line scan along x (i.e. $I_C(x,y=0) \Rightarrow I_C(x)$) leading to Equations 5 and 6 in the main text.

Image Collection, Analysis and Line-Profile Fitting

Division of the TIRF and EPI Intensity Profiles

The intensity profile for the TIRF image (Figure 2B) is plotted against the inferred z distance (based on the microtubule tilt angle). It is then divided by the EPI-excitation intensity profile of the same microtubule, normalised to unity (Figure 2C) to account for the microscope collection efficiency function.

The EPI intensity profile is obtained from data taken in the EPI z-stack recorded to determine the microtubule tilt angle (see Equipment and Methods). The z-plane corresponding to the plane of focus for the TIRF image is identified and averaged with the adjacent planes above and below. As can be seen the EPI intensity profile varies strongly with height – despite the uniformity of the excitation in z – emphasising the need for correction of the TIRF intensity profile.

To divide the intensity profile obtained from TIRF-illumination with that from EPI-illumination, both intensity profiles are aligned at the left edges (corresponding to the microtubule end nearest the coverglass surface - this was occasionally necessary as slight movements of 1 or 2 pixels in microtubule position were sometimes observed between TIRF and EPI images). Similarly, it was ensured that for both EPI and TIRF, the measured intensity profiles had the same spacing (resolution) and were started well before the microtubule and extended until long after its end.

Possible Sources of Error

Errors in the determination of the penetration depth could be introduced by fluorescence bleaching of the labelled microtubules during the TIRF image acquisition as well as by microtubule depolymerisation. To rule out these effects, after taking the complete set of images for six different AOI, the AOI was set back to its first value and the microtubule was re-imaged. Shown in supplementary Figure S1 are the intensity profiles obtained from these two images. The agreement between the two profiles is good, demonstrating that no significant bleaching or microtubule depolymerisation has occurred. Furthermore, this effectively demonstrates the reproducibility in selecting the AOI.

EPI illumination is Pseudo-Uniform in *z*

We assume that EPI illumination is equivalent to uniform illumination (i.e. for EPI $I_{ex}^{EPI}(z) = \text{constant}$). To demonstrate this, a intensity profile along a very steeply tilted (~15.9º) microtubule was recorded (Figure S2). Images were then recorded of this microtubule, first using illumination provided by the TIRF laser (but with an AOI of 0°) and second using standard arc-lamp based EPI illumination. This method of laser illumination, where a large (~mm diameter) collimated beam propagates along the optical axis, is assumed to be a good approximation to uniform (in z) light. Intensity profiles along the long axis of these microtubules with the two illumination methods were almost indistinguishable, suggesting that EPI illumination is similar to uniform illumination over the length scales of interest.

Determination of microtubule tilt angle.

An EPI *z*-stack was recorded of each tilted microtubule (50 nm step size, typically over 10 μm total height to capture the entire microtubule). Using software written in Igor Pro 6 (Wavemetrics, Oregon, USA) maximum projections in 3 orthogonal directions (*z*, *x* and *y*) were then produced (Figure S3, A, B and C, respectively). In the *z* projection (*i.e* the projection onto the *x*-*y* plane) a line was drawn along the central axis of the microtubule, allowing calculation of its angle, θ_z, with respect to the *x*-axis (Figure S3, A). In either the *x* or *y* projection, where the central long axis of the microtubule was sometimes less clear due to axial blurring, multiple intensity profiles along the *z* axis were determined that bisected the microtubule along its entire length (three examples are shown in Figure S3, D corresponding to the three lines in Figure S3, C). Lorentzian functions were then fit to these intensity profiles. The peak positions of the Lorentzian functions (corresponding to the z position of the microtubule) were then plotted versus either *x* or *y* position (Figure S3, E). The slopes of these plots give the tangent of the angles θ_y and θ_x. One can then calculate two estimates of the 'apparent' tilt angle θ_{tilt}, using θ_z and either θ_y or θ_x by using $\theta_{tilt} = \arctan(\cos\theta_z \tan\theta_y)$ or $\theta_{tilt} = \arctan(\cos(90 - \theta_z)\tan\theta_x)$. Here we used the average of the two values.

Using the TIRF objective to image microtubules in an aqueous environment results in inherent axial aberration (Hell *et al*., 1993). This will lead to an incorrect determination of the tilt angle of the microtubule and consequently to an error in the determined penetration depth. The degree of this effect was determined by measuring the apparent tilt angle for *the same* tilted microtubule first with a water immersion objective, where axial aberrations are almost eliminated (Zeiss, 63x NA 1.2, with coverglass thickness correction collar), and then the objective used for TIRF microscopy. In a first order approximation a correction factor (that can be used to derive the true tilt angle from the TIRF-objective measured apparent tilt angle) is given by the ratio of the angles obtained in both analyses. We determined a correction factor of 0.82 from measuring 8 microtubules, covering an angular range of tilt from 0.5 ° - 10 °. This value is in good agreement with the scaling factor of 0.83 given in (Hell et al., 1993) for an oil-immersion objective of NA=1.3 operated in aqueous solution.